Tissue Engineering and Regenerative Medicine

A novel filtration system for point of care washing of cellular therapy products

SCHOLARONE™
Manuscripts

A novel filtration system for point of care washing of cellular therapy products

Rui Tostoes[1], John R. Dodgson[2], Ben Weil[1], Spyridon Gerontas[1], Chris Mason[1], Farlan Veraitch[1]

1 – The Advanced Centre for Biochemical Engineering, Department of Biochemical Engineering, University College London, Bernard Katz Building, Gower Street, London WC1H 0AH, UK

2 – Dodgson Associates Ltd., London, UK

23 **Abstract**

24

25 The cell therapy industry would greatly benefit from a simple point of care solution to remove

26 Dimethyl Sulfoxide (DMSO) from small volume thawed cell suspensions prior to injection. We have

27 designed and validated a novel dead-end filtration device, which takes advantage of the higher density

28 of thawed cell suspensions to remove the DMSO and protein impurities from the cell suspension

29 without fouling the filter membrane. The filter was designed to avoid fluid circuits and minimize the

30 surface area that is contacted by the cell suspension, thus reducing cell losses by design.

31 The filtration process was established through optimization of the fluid flow configuration, backflush

32 cycles and filter geometry. Overall, this novel filtration device allows for a 1 mL of thawed

33 cryopreserved cell suspensions, containing 10^7 cells of a foetal lung fibroblast cell line (MRC-5), to

34 be washed in less than 30 minutes. More than 95% of the DMSO and up to 94% of the Albumin-

35 Fluorescein-Isothiocyanate content can be removed while the viable cell recovery is higher than 80%.

36 We have also demonstrated that this system can be used for bone marrow-derived human

37 mesenchymal stem cells with more than 73% cell recovery and 85% DMSO reduction. This is the first

38 time that a dead end (normal) filtration process has been used to successfully wash high density

39 human cell suspensions. In practice, this novel solid-liquid separation technology fills the need for

40 small volume washing in closed processing systems for cellular therapies.

41

42

1. Introduction

The cryopreservation of cellular therapy products is usually performed by controlled-rate freezing (1-5°C/min) in the presence of DMSO, which is the prefered cryopreservation agent (CPA) in virtually every cryopreservation solution (Rowley 2009). This is due to its efficient diffusion across the cell membrane coupled with the ability to prevent intracellular ice formation and osmotic stress during slow rate freezing (Mazur 1984). In the treatment of blood disorders the cell product may be infused to patients without any reduction in DMSO concentration even though the presence of this CPA has been shown to cause nausea, vomiting, cardiac arrhythmia (Cox et al. 2012) and, less frequently, more severe adverse reactions such as neurotoxicity (Abdelkefi et al. 2009), cardiac arrest or epileptic seizure (Cox et al. 2012). Thus, safety concerns are raised when the cellular product consists of a small volume (<10 mL) cell suspension which will be injected into a solid tissue such as the brain or heart (FDA 1997). Such an injection is likely to expose the patient's cells to a much higher DMSO concentration than a blood stream infused product. Although there is no safety data for concentrated DMSO injections in humans, there is published work in animals (Galvao et al. 2014) and brain tissue culture (Tamagnini et al. 2014). These data strongly suggest that a reduction in DMSO concentration is required for cell therapies which are administered via injection into solid tissues and should be performed even in infused cell therapies.

To reduce the DMSO concentration in thawed cell suspensions the most common process is open lab centrifugation. This process is only acceptable in a laminar flow chamber placed in a grade B cleanroom background, which represents an unacceptable financial burden for the current Point of Care (POC) sites such as hospitals or clinics that do not have a cell-processing facility. Another solution is the use of closed centrifugal systems such as the COBE 2991 (Terumo BCT, Colorado, USA) or Sepax S-100 devices (Biosafe S.A., Eysins, Switzerland). These can be used to separate mononuclear cells from red blood cells or as cell washing devices, reaching 97% removal of the DMSO content (Rodríguez et al. 2004) and a total nucleated cell recovery of 75% in cryopreserved peripheral blood progenitor cell products for autologous infusion (Sánchez-Salinas et al. 2012). While these centrifuge-based systems are efficient, they are expensive and not amenable to small scale cell

70   processing. Hanna and colleagues have described a microfluidic device which removes up to 70% of

71   the initial DMSO concentration from fresh cell suspensions spiked with the cryoprotectant in a three-

72   stream diffusion system (Hanna et al. 2012). The post-wash viable cell recovery reported by these

73   authors was above 95%. Recently, a dilution-filtration system has been reported by Zhou *et al*. This

74   system relies on a tangential flow filtration system (TFF) which enables the removal of 93% of the

75   CPA (glycerol in this instance) from thawed human red blood cells with a viable cell recovery of 91%

76   (Zhou et al. 2011). The main disadvantage of TFF based methods is that they are mostly used for

77   volumes starting at hundreds of mL or litres, and any scale down design of a TFF will include an

78   external circuit where cells are likely to be lost either by liquid adsorption to the material or shear

79   (Jaouen et al. 1999; Kuo et al. 2010). Overall, there is an unmet need for a small scale solid-liquid

80   separation technologies which are cost-effective, simple to operate and enable a high cell recovery.

81   In this work, we have designed and validated a novel dead end filtration device for the removal of

82   DMSO from 1 mL thawed cell suspensions. A typical dead-end filtration operation produces an

83   exponential pressure increase in the retentate chamber due to the progressive membrane clogging by

84   the retained cells (Rushton et al. 2000; Xu and Chellam 2005). However, it is also a simple system

85   with no moving parts and thus amenable to become a cost-efficient closed point of care solution for

86   cell washing. The location of the filter membrane on top of the cell suspension and the non-turbulent

87   flow allowed the thawed cell suspension to form a bed at the bottom of the filter device and limit the

88   contact of the cells with the filter membrane, thus enabling the dead end filtration to progress for long

89   enough to remove more than 95% of the DMSO. This device was also designed to have a minimal

90   contact area with cells, to avoid cell losses due to liquid adsorption into long fluidic circuits. With this

91   minimal surface area approach the viable cell recoveries were above 80%, after the filtration of

92   thawed 1mL cell suspensions.

93   **2.   Materials and Methods**

94   2.1. Cell culture and cryopreservation

95   The human lung fibroblast cell line MRC-5 (ATCC Catalog No. CCL-171) was used as a model cell

96   line throughout this work. These cells were cultured for a maximum of 40 population doublings (PD)

97   as these cells can reach 42 PD without senescence, according to the supplier. The cells were cultured

4

98   in Eagle's Minimum Essential Medium (EMEM, M5650 Sigma-Aldrich UK) supplemented with 10%

99   Foetal Bovine Serum (FBS, Seralab UK), 1% Glutamine and 1% MEM Non-Essential Amino Acids

100   (NEAA, GIBCO, UK) using Nunc T-flasks with 175 cm^2 surface area (Thermo Scientific, UK). Bone

101   Marrow-derived human Mesenchymal Stromal Cells (hMSC) from 2 different donors were purchased

102   from Lonza (Poietics^{TM} human mesenchymal stem cells) and cultured in complete growth medium:

103   DMEM low glucose (21885-025, Life Technologies, UK) supplemented with 10% FBS, 1% NEAA

104   and 1 ng/mL recombinant human basic Fibroblast Growth Factor (bFGF, R&D Systems, MN, US).

105   The hMSCs were cultured for expansion up to passage 7, to minimize the senescence of the

106   population and used as a cell therapy-relevant model to validate the filtration system developed in this

107   work. The hMSC were differentiated using GIBCO® StemPro reagents (GIBCO,UK): For

108   adipogenic, chondrogenic and osteogenic differentiation, hMSCs were seeded into 12-well plates at 1

109   x 10^4 cells/cm^2, 1.6 x 10^7 cells/mL 10 μL droplets and 5 x 10^3 cells/cm^2, respectively. After 24h in

110   culture in complete growth medium, the media was discarded and 1 ml of Adipogenesis,

111   Chondrogenesis or Osteogenesis Differentiation Medium (StemPro Differentiaiton Kit, GIBCO,

112   Invitrogen) were added to each well. Medium was fully exchanged every 3 days and at day 21 cells

113   were washed in 1X PBS and fixed at room temperature, with 4% paraformaldehyde (PFA), for 10

114   minutes for adipogenesis cultures and 30 minutes for chondrogenesis and osteogenesis cultures. For

115   adipogenesis cultures, 60% isopropanol was added to the cells and let sit for 5 minutes. Cells were

116   then stained with a filtered solution of 0.3% w/v Oil Red O/isopropanol in distilled water 3:2 for 5

117   minutes, rinsed under tap and counterstained with hematoxilin for 1 minute. For chondrogenesis

118   cultures, 1% Alcian Blue solution prepared in 0.1M HCl was used to stain the chondrocytes. After 30

119   minutes, cells were rinsed twice in 0.1M HCL and then under running tap water. For osteogenesis, .

120   2% Alizarin Red S solution (pH 4.2) was added for 5 minutes and then the wells were carefully rinsed

121   with distilled water to avoid the micromasses disruption.

122   For cryopreservation, cells were exposed to Trypsin (Sigma-Aldrich, UK) for 5 min at 37 °C and the

123   reaction was stopped by adding 2 volumes of EMEM (supplemented with 10% FBS) per volume of

124   trypsin. The resulting cell suspension was centrifuged at 300g for 5 min at room temperature, washed

125   with PBS and centrifuged again under the same conditions. The washed cell pellet was resuspended in

5

126   cold (2-8 °C) CryoStor™ containing 5% v/v of DMSO (CS5, BioLife Solutions, WA, USA) to yield 1

127   mL single cell suspension containing 10-20 million cells/mL. This cell suspension was dispensed into

128   3 mL Crystal™ vials (Aseptic Technologies, Belgium), incubated for 10 minutes on ice and then

129   transferred to a -80 °C freezer where it was cooled at an approximate rate of -1 °C/min, using a

130   CoolCell container (BioCision, CA, US) and kept up to a maximum of 1 month before use.

131   2.2. Device design and operation

132   The filter devices were designed using AutoCad 2011 (Autodesk, CA 94903, USA) and manufactured

133   by machining in UCL's Biochemical Engineering workshop, using either Poly(methyl methacrylate)

134   (PMMA) or Stainless Steel 316 (SS) as a the base material, and by injection molding using the

135   Protomold service from Protolabs, UK. The base material used for injection molding was Cyclic

136   Olefin Co-polymer (COC).

137   All the devices were designed to allow the 1 mL thawed cell suspension to form an undisturbed bed

138   while the washing buffer flowed through the cell suspension. This configuration minimized and

139   delayed the progressive filter clogging typical in a dead end filtration process. The design shown in

140   Figure 1A enabled the formation of this cell bed by localizing the filter membrane above the cell

141   suspension and ensuring that the lower chamber had a higher volume than that same loaded cell

142   suspension, such that during the wash operation there was a decreasing cell concentration from the top

143   surface of the cell bed to the filter membrane (Figure 1B, top). The wash step was performed by

144   flowing wash buffer (PBS) from the bottom and lateral inlets of the lower chamber (Figure 1B, top).

145   The semi-conical shape of this chamber was designed to enable the post wash gas phase volume

146   reduction of the cell suspension: this shape stabilizes an injected air bubble which occupied the top

147   part of the bottom chamber, leaving behind a volume reduced cell suspension (Figure 1B, middle) that

148   was collected directly into a syringe (Figure 1B, bottom); these process steps are shown in the

149   supplementary movies S1-3 (A with dye and B with cells) and S4. The fixed process inputs and

150   parameters are listed in Table I; the operating temperature was kept at 21 ± 2°C.

151   2.3. Cell counts

152   The cell numbers and viability were counted using a Vi-CELL Cell Viability Analyser (Beckman

153   Coulter, UK) before and after the cell suspension processing. The results are shown as percent viable

6

154 cell recovery (VCR) and correspond to the ratio between total viable cells after processing and total

155 viable cells before processing.

156   2.4. <u>DMSO measurement</u>

157 The concentration of DMSO in the filtrate and retentate was measured by reverse phase high

158 performance liquid chromatography (HPLC) using an Agilent 1200 series device (Agilent

159 Technologies UK Limited) under the control of the Agilent Chemstation software. A 4 mm x 125 mm

160 (internal diameter x length) Nucleosil C18 column with a particle size of 5 μm (Sigma-Aldrich, UK)

161 was used as the stationary phase, while the mobile phase was based on a previously published

162 protocol (Thumm et al. 1991). Briefly, an aliquot was taken from the filtrate or retentate sample and

163 diluted 1:20 in 0.1% (v/v) Trifluoro Acetic Acid (TFA, Sigma-Aldrich UK). Calibration curves of CS

164 5 were prepared at the appropriate dilution and analyzed in parallel with the samples. The elution

165 profile consisted of 100% distilled water in the first 5 min followed by a linear gradient of

166 water/acetonitrile until 100% of acetonitrile was reached at 7 min; the reverse gradient was applied to

167 reach 100% water at 9 min and maintained until 15 min. The DMSO peak was detected (210 nm

168 detection wavelength) at 3-5 min of elution time. All results are presented as the ratio $\frac{C}{C_0}$, where C and

169 C_0 are the final and initial concentration of DMSO, respectively.

170   2.5. <u>FITC-Albumin experiments and quantification</u>

171 To assess the removal of larger molecular weight molecules, 20 μL of conjugated Albumin-

172 Fluorescein Isothiocyanate (FITC) (A9971, Sigma UK) at a concentration of 5 mg/mL in CS 5 were

173 added to the 1 mL cell suspension immediately after thaw and before the filtration process. The

174 Albumin-FITC concentrations were measured using a FluoStar Optima microplate reader (excitation

175 450 nm, emission 544 nm). Calibration curves of Albumin FITC in CS 5 were prepared at the

176 appropriate dilution and analyzed in parallel with the samples. All results are presented as the ratio $\frac{C}{C_0}$,

177 where C and C_0 are the final and initial concentrations of FITC-Albumin, respectively.

178   2.6. <u>Pressure Measurements</u>

179 The pressure in the lower chamber of the system was measured against the atmospheric pressure using

180 either a manual or a digital manometer with data-logging capabilities (Sper Scientific, AZ US).

7

181   2.7. <u>Filtration model</u>

182 A modified form of the diafiltration equation was used to model and predict solute removal from the

183 cell suspensions:

$$\frac{C}{C_0} = e^{-\frac{F \times t}{V_c} \times k} = e^{-N \times k} \qquad\qquad \text{Equation 1}$$

184 where F is the flow rate in mL/min, t is time in min, V_C is the lower (cell-containing) chamber

185 volume, N is the number of diavolumes, defined as the quocient between the total volume used for

186 filtration and the volume of the filtration chamber, and k is a wash efficiency parameter which is

187 dependent on the geometry of the device.

188   2.8. <u>Computational Fluid Dynamics</u>

189 The commercial software package COMSOL Multiphysics 5.0 (Hatfield, Comsol, UK) was used to

190 simulate the velocity, pressure and DMSO profiles in the filter device. The laminar flow application

191 mode within the COMSOL Multiphysics software was chosen to simulate the velocity and pressure,

192 whereas the mass transfer for diluted species application mode was chosen to simulate the DMSO

193 profile. To lower the computer memory requirements of the overall simulation, the flow field is

194 simulated first as the viscosity and densities of the culture medium containing DMSO are considered

195 constant (relatively low species concentration). The solved flow field is then saved and coupled with a

196 mass transfer model, which describes DMSO convection/diffusion in the filter device.

197 In all simulations, the boundaries of the filtering device were meshed with 52155 triangular elements

198 (extra fine mesh; default settings) and its domain with 376906 quadrilateral elements (normal mesh

199 option; default settings) using the free mesh option of COMSOL Multiphysics's mesh generator. The

200 number of degrees of freedom was 377702. The convergence was tested by a two-fold increase in the

201 number of elements. The velocity, pressure and DMSO concentration simulated by using the new

202 mesh were agreed at the three significant figures level with the velocity, pressure and DMSO

203 concentration simulated by using the default mesh. The simulation results are presented as contour

204 plots, blue represents areas of low DMSO concentration and red represents areas of high values for

205 DMSO concentration.

206   2.9. <u>Flow Cytometry</u>

8

207 The post filtration multipotency of the hMSCs was assessed using an hMSC phenotyping kit

208 (Miltenyi Biotec, Surrey, UK) flow cytometry assay. Briefly, single cell suspensions, following wash

209 and volume reduction using the novel filtration device, were equally divided into 7 samples.

210 Antibodies were diluted 1:11 in 110ul buffer per 1x106 cells and incubated with the samples on ice

211 for 30 minutes. The 7 samples for each MSC test consisted of 4 single fluorophore controls (CD105-

212 PE, CD90-FITC, CD73-APC, CD14-/CD20-/CD34-/CD45-PerCP) for compensation, a cell only

213 sample (incubated with 110ul FACS buffer, also for 30 minutes on ice), the Isotype Control Cocktail

214 and the MSC Phenotyping Cocktail provided in the MSC phenotyping kit (Miltenyi). After antibody

215 labelling, cells were washed and re-suspended in 0.5ml FACS buffer in flow analysis tubes (BD

216 Bioscience, Oxford, UK). Flow cytometery was performed using a BD LSR II flow cytometer. For

217 analysis, at least 50,000 events were initially gated based on forward and side scatter and forward

218 scatter height against area was used for doublet removal. The isotype control cocktail was run with the

219 same gating strategy and MSCs defined from gating the top 1% of isotype expression. To confirm an

220 MSC phenotype, greater than 95% expression of CD105, CD90, CD73, and less than 2% expression

221 of CD14, CD20, CD34 and CD45 must be observed (Dominici et al. 2006). N=3 samples were run

222 and the standard deviation calculated.

223   2.10.   <u>Statistics</u>

224 The statistical analysis was performed using the Excel data analysis add-on and the GraphPad

225 software. The p-values presented were calculated for the two tails of the normal distribution and when

226 more than 2 groups were compared Tukey's multicomparison test was used. The notation "n"

227 (lowercase, not to be mistaken by uppercase "N", the diavolumes) was used to denote the number of

228 independent replicates.

229 **3. Results**

230 To test this new filtration device it was necessary to choose a filter medium and a pore size which

231 minimized the rate of pressure increase during the wash operation; initial tests demonstrated that a

232 hydrophilic Polyvinylidene fluoride (hPVDF) with a nominal pore size of 0.65 μm was a feasible

233 starting point (data not shown).

234 To maximize the number of cells recovered, it was hypothesized that a backflush step between the

235 wash and concentration steps would dislodge cells from the filter membrane and increase the post

236 process VCR. The wash step was performed using a flow rate of 2 mL/min via the bottom inlet and 5

237 mL/min through the lateral inlet (2/5 flow). While no significant difference in VCR was observed

238 when this backflush step was present (compared to its absence), there were significant effects on the

239 amount of solute removed. Figure 2A depicts the DMSO concentration in the filtrate over time, and it

240 is visible that after the backflush step there is an increase in the DMSO concentration in the filtrate. It

241 was hypothesized that the overall DMSO removal of the retentate could be enhanced if several

242 backflush steps were applied during the wash phase. Figure 2B depicts the experimental design used

243 to test this hypothesis, where 3 backflush steps were performed during a 2/5 wash for 10 min (3x

244 backflush) and compared with a 10 min 2/5 wash with one backflush step after the wash operation (1x

245 backflush). Figure 2C shows that the 3x backflush wash yielded a lower DMSO concentration than

246 the 1x backflush wash, with 0.136 ± 0.003 and 0.20 ± 0.01 of the initial DMSO concentration,

247 respectively (n=3, p<0.001). This increase in DMSO removal was also associated with a higher lower

248 chamber pressure in the 3x backflush wash when compared with the 1x backflush wash, after 10

249 minutes, as shown in Figure 2D.

250 The individual contributions of the bottom and lateral flows for the DMSO removal from the cell

251 suspension were investigated. Figure 3 shows that, after a 10 minutes wash period, the lateral flow

252 reduces the initial amount of DMSO to 0.66 ± 0.09 (n=5) of its initial concentration. There was no

253 significant difference between the concentration of DMSO after the bottom flow wash and the

254 lateral+bottom (2/5) flow wash (0.25 ± 0.01, n=3 and 0.17 ± 0.06, n=3), for the 10 min wash period.

255 However, the presence of a bottom flow results in a significantly higher DMSO reduction when

256 compared to using lateral flow only (p<0.01).

257 The combinatorial effect of the lateral and bottom flows (2/5 flow) on DMSO reduction was further

258 investigated as a function of the diavolumes N (Bottom Flow x Time), as shown in Figure 4A. The

259 curve corresponding to the 2/5 flow is in agreement with the diafiltration equation, with the wash

260 efficiency value k being constant (R^2=0.998); without the lateral flow, the bottom flow curve deviates

261 from Equation 1, yielding lower DMSO reduction values. These differences correlate with different

10

262   pressure profiles (Figure 4B): the lateral flow of PBS leads to an increased pressure ending in 80

263   mbar, whereas pressure in the bottom flow configuration is kept at 20 mbar or less.

264   To be useful as part of a point of care device, this filter will be manufactured as an injection molded

265   part, like most medical devices or bioprocessing consumables. The panels C and D in Figure 4 depict

266   a PMMA filter device which houses an injection molded (IM) COC lower chamber whose shape is

267   identical to the one in Figure 1A. This IM device was used to process thawed MRC-5 cell suspensions

268   at 2 mL/min bottom flow, without lateral flow, for 24 min and the volumes, cell concentration and

269   DMSO removal are shown in Table 2. The DMSO reduction for this data was 91 ± 2% for N=32, as

270   shown in Figure 4A. The cell recovery and volume reduction was 84 ± 1% and 2.7 ± 0.5 fold,

271   respectively. These results demonstrate that this filtration system can be successfully used for small

272   volume cell suspension wash and volume reduction, with a cell recovery of more than 80%.

273   Moreover, the use of a thermoplastic material indicates that the performance of the PMMA device is

274   close to the performance of the consumable.

275   The filtration device was redesigned to increase the DMSO reduction while avoiding pressure build-

276   up in the lower chamber, i.e. increasing the wash without using the lateral flow. Figure 5A shows the

277   3 geometries of the filtration device, where M1 (mark 1) is the original design, with a lower chamber

278   height (bottom inlet to filter membrane) of 0.8 cm and a filtration area of 3.5 cm^2. To minimize the

279   diffusional distances and increase the fluid velocity, the M2 geometry was designed to increase the

280   height of the chamber by 50% (compared to M1) while maintaining a constant volume, thus

281   decreasing the cross sectional area of the bottom flow chamber. This was achieved by changing the

282   chamber from a round bottom to a V-bottom shape. Computational fluid dynamics (CFD) was used to

283   model DMSO removal in M2 under the 2/5 flow configuration; the surface plot in figure 5B depicts

284   the top view of the M2 device and it indicates that there is accumulation of DMSO in the outer area of

285   the membrane. Again, these areas are the furthest away from the bottom flow jet and they could be

286   designed out (or "trimmed" out) of the M2 geometry thus yielding the M3 geometry, with a 2.5 cm^2

287   area (30% decrease vs M2) and a lower chamber height of 1.5 cm (25% increase vs M2). These

288   geometry changes had significant effects on the DMSO removal rate, as demonstrated in Figure 5C.

289   When using only the bottom inlet to flow wash buffer through the cell suspension (solid lines) it is

11

290   visible that the amount of DMSO removed per diavolumes of buffer increases from M1 to M3. Unlike

291   the M1 and M2 bottom flow curves, the M3 curve fits a single exponential line as described in

292   Equation 1 (solid line, R^2=0.97); likewise, when the lateral flow is used for the M1 and M2

293   geometries, their DMSO reduction curves also fit a single exponential decay (solid lines, R^2=0.97 for

294   both). However, the M3 geometry, operating with bottom flow only, sustains the lower chamber

295   pressure below 15 mbar, whereas the M1 and M2 geometries, operating with the 2/5 flow, can reach

296   pressures of 100 and 400 mbar, respectively (Figure 5D, n=3). These data indicate that the M3

297   geometry enables an efficient DMSO reduction while operating at low pressures.

298   To further validate the hypothesis that the diffusional distance is the critical factor behind these

299   increases in efficiency from M1 to M3, the differences in these geometries were factored into

300   Equation 1. By keeping the volume of the chamber constant and increasing the height of the chamber,

301   the whole shape becomes "thinner" along its length thereby reducing the diffusional distance and

302   increasing the fluid velocity. As such, the increase in height is proportional to the increase in the

303   amount of DMSO removed. To incorporate this into equation 1 it should be noted that the effect of the

304   height implies that for the same level of DMSO removal, less diavolumes (N) are needed as the height

305   is increased. In this way, N should be replaced by the product N×height. However, since this is an

306   exponential term it must be dimensionless. Since N is dimensionless so should the height be; to

307   achieve this it was noted that height=sin(α)×longer slope (as per figure 5E) and the sin(α) was used

308   instead of the height. Thus, Equation 1 can be modified to:

$$\frac{C}{C_0} = e^{-\frac{Ft}{V_c}k\sin\alpha} = e^{-Nk\sin\alpha} \qquad\qquad \text{Equation 2}$$

309   The semi-logarithmic plot of $\frac{C}{C_0}$ vs $N \times \sin\alpha$ is depicted in Figure 5F. This plot shows that the data

310   points derived from Equation 1 in Figure 5C (M1 and M2 with lateral flow and M3 with bottom flow)

311   can be modelled by a single curve using Equation 2 (R^2=0.98).

312   The M3 geometry was further characterized by its ability to reduce the amount of a model protein,

313   albumin-FITC; After a 32 diavolumes wash the initial concentration of this protein was reduced by 94

314   ± 1% (Figure 5G). Furthermore, the viable cell recovery using M3 was 94 ± 5%, thus confirming that

315   this geometry also enables a high cell recovery, while the volume reduction was 1.55 ± 0.08 fold

316   (Table 2). To assess the functionality and long-term viability of the cells after being processed, the

317   M3 geometry was manufactured in stainless steel 316. Figure 5H demonstrates that, after a 16

318   diavolumes wash, the MRC-5 cell line still grows at the same specific rate as fresh cells or cells which

319   have also been thawed but processed using a bench top centrifuge (see methods). Importantly, cell

320   counts after a 24 hour culture showed that after thawing, processing and plating $62 \pm 15\%$ of the cells

321   (post thaw counts) survived; when no cell processing was performed and cells were directly plated in

322   adherent flasks, the cell recovery was $58 \pm 5\%$ (n=4).

323   To validate this geometry for cell therapy applications, hMSCs were processed using the M3

324   geometry filtration device. The post filtration characterization of these cells was performed according

325   to the ISCT criteria (Dominici et al. 2006) and the 3 cell runs (generated from 2 donors) showed that

326   hMSCs retained their characteristic surface markers (Figure 6 A and B), while retaining their ability

327   to adhere to plastic, proliferate (Figure 6E and F) and the capability for chondrogenic, osteogenic and

328   adipogenic differentiation (Figure 6G, H and I). The viable cell recovery after these 3 runs ranged

329   from 73 to 99%, while the DMSO removal ranged from 86-88% (Figure 6 C and D).

330   **4. Discussion**

331   In this work, we have designed and characterized a filtration system to process thawed cell

332   suspensions which removes more than 90% of the DMSO and recovers more than 80% of the viable

333   cells. Most importantly, this filtration system does not require an outside loop like a TFF system, thus

334   minimizing the shear stress that cells are exposed to and the area where liquid can be lost by

335   adsorption.

336   The central element of the filter housing design (Figure 1A) is the laminar flow that is established at

337   these dimensions and flow velocities. While it is visible that the cell suspension has settled at the end

338   of the filtration process, it is unlikely that cell settling can be faster than the flow rate of wash buffer

339   from the bottom inlet. The average linear velocity of wash buffer crossing the membrane from the

340   bottom flow is 0.57 cm/min while the average cell settling velocity is at least one order of magnitude

341   below this velocity (Chalmers et al. 1999). Another possibility is that the settling velocity of the cells

342   is increased in the Cryostor media; while this is true in absolute terms, because the CS5 is hypertonic,

343   it is the density difference between the cells in CS5 and the CS5 medium that is relevant for the

344   settling velocity. Thus, it is expected that the density differences between fresh cells in PBS and

345   thawed cells in CS5 are the same; this was confirmed by an isopycnic centrifugation using a Percoll

346   gradient (Supplementary Figure 1) which confirmed that the density of the MRC-5 cells in CS5 is

347   between 1.04 and 1.06 g/mL, whereas the literature reports a similar density for these cells in PBS

348   (1.05 g/mL) (Birnie and Rickwood 1980).

349   Using the lateral flow configuration, the DMSO concentration was reduced to 0.66 of its initial value

350   (Figure 4); interestingly, this value is the same as the ratio of the cell suspension volume to the lower

351   chamber volume (1mL/1.5mL), which strongly suggests that the lateral flow alone does not remove

352   any significant amount of DMSO after 10 minutes. Nevertheless, the addition of lateral flow to the

353   bottom flow (2/5 flow) seems to provide a more efficient mixing for both M1 and M2 geometries, and

354   thus a better reduction in DMSO concentration, when compared with using the bottom flow only

355   (Figure 5C). These results follow the same trend as the use of increased backflush cycles to enhance

356   DMSO reduction (Figure 2), also at the expense of higher pressure differences. Taken together, these

357   two data sets strongly suggest that both the lateral flow and the backflush cycles increase the DMSO

358   removal, by dispersing the cell bed that is established if bottom flow only is used. The design changes

359   that lead to the M3 geometry had the goal of avoiding the dispersion of the cell bed that results in

360   increased lower chamber pressures This was accomplished by prioritizing the minimization of the

361   average diffusional length and the maximization of the fluid velocity. The M3 geometry, while having

362   a lower volume reduction capability when compared to M1, does not require lateral flow to have a

363   single exponential wash profile, as described by equation 1, while washing more than 95% of the

364   DMSO using less diavolumes; using only one inlet to flow the wash buffer makes the operation

365   simpler and will decrease the manufacturing cost of the POC device. The empirical model described

366   by Equation 2 validates the aforementioned design hypothesis, as depicted in Figure 5F; when the

367   DMSO removal curve fits equation 1, the different geometries can be normalized to the distance

368   between the filter membrane and the bottom flow inlet. Both the M1 and M2 geometries DMSO

369   removal data points shift to the right of the curve in Figure 5F when only bottom flow is used, a result

370   which can be explained by cell settling in a low shear environment. The M3 filtration device was also

14

371 shown to remove up to 94% of a model protein, Albumin-FITC (Figure 5 G); this ability to removes

372 higher molecular weight contaminants from cell suspensions can be of high value when the whole cell

373 therapy process is considered.

374 The processing of hMSCs (Figure 6) demonstrated the capability of this novel filtration device for

375 small volume cell wash, using cells relevant for cell therapy. Despite the DMSO removal efficiency

376 being lower than for the MRC-5 cells wash, 88% of the DMSO was removed from hMSC cell

377 suspensions. This lower washing efficiency can be attributed to different biophysical characteristics,

378 namely cell size, and it is a clear area of research in the development of this technology. Another

379 point for future research is how to have sterility as a release criterion for the cellular therapies, since

380 this takes about 24h to be tested and the therapies need to be administered within minutes.

381 In a broader sense, a simple solid-liquid separation device for small volumes is a key enabling

382 technology to make the distributed manufacturing of cellular therapies possible.

Acknowledgments

Competing financial interests

397 **5. Bibliography**

398   Abdelkefi A, Lakhal A, Moojat N, Hamed LB, Fekih J, Ladeb S, Torjman L, Othman TB. 2009.

399   Severe neurotoxicity associated with dimethyl sulphoxide following PBSCT. Bone Marrow

400   Transplant. England. p 323-4.

401   Birnie G, Rickwood D. 1980. Centrifugal Separations in Molecular and Cell Biology. Journal of Basic

402   Microbiology 20(2):153.

403   Chalmers JJ, Haam S, Zhao Y, McCloskey K, Moore L, Zborowski M, Williams PS. 1999.

404   Quantification of cellular properties from external fields and resulting induced velocity:

405   cellular hydrodynamic diameter. Biotechnol Bioeng 64(5):509-18.

406   Cox MA, Kastrup J, Hrubisko M. 2012. Historical perspectives and the future of adverse reactions

407   associated with haemopoietic stem cells cryopreserved with dimethyl sulfoxide. Cell Tissue

408   Bank 13(2):203-15.

409   Dominici M, Le Blanc K, Mueller I, Slaper-Cortenbach I, Marini F, Krause D, Deans R, Keating A,

410   Prockop D, Horwitz E. 2006. Minimal criteria for defining multipotent mesenchymal stromal

411   cells. The International Society for Cellular Therapy position statement. Cytotherapy

412   8(4):315-7.

413   FDA. 1997. Food and Drug Administration Guidance for Industry - Q3C Impurities: Residual

414   Solvents.

415   Galvao J, Davis B, Tilley M, Normando E, Duchen MR, Cordeiro MF. 2014. Unexpected low-dose

416   toxicity of the universal solvent DMSO. Faseb j 28(3):1317-30.

417   Hanna J, Hubel A, Lemke E. 2012. Diffusion-based extraction of DMSO from a cell suspension in a

418   three stream, vertical microchannel. Biotechnol Bioeng 109(9):2316-24.

419   Jaouen P, Vandanjon L, Quéméneur F. 1999. The shear stress of microalgal cell suspensions

420   (Tetraselmis suecica) in tangential flow filtration systems: the role of pumps. 68(2):149–154.

421   Kuo JS, Zhao Y, Schiro PG, Ng L, Lim DS, Shelby JP, Chiu DT. 2010. Deformability considerations

422   in filtration of biological cells. Lab Chip 10(7):837-42.

423   Mazur P. 1984. Freezing of living cells: mechanisms and implications. Am J Physiol 247(3 Pt

424   1):C125-42.

425   Rodríguez L, Azqueta C, Azzalin S, García J, Querol S. 2004. Washing of cord blood grafts after

426   thawing: high cell recovery using an automated and closed system*. Vox Sanguinis

427   87(3):165-172.

428   Rowley S. 2009. Hematopoietic Stem Cell Cryopreservation: A Review of Current Techniques.

429   Journal of Hematotherapy 1(3):233-250.

430   Rushton A, Ward A, Holdich R. 2000. Solid-liquid filtration and separation technology. New York:

431   Wiley-VCH: Weinheim. 587 p.

432   Sánchez-Salinas A, Cabañas-Perianes V, Blanquer M, Majado M, Insausti C, Monserrat J, Sánchez-

433   Ibáñez M, Menchón P, García-Hernández A, Gómez-Espuch J and others. 2012. An

434   automatic wash method for dimethyl sulfoxide removal in autologous hematopoietic stem cell

435   transplantation decreases the adverse effects related to infusion. Transfusion 52(11):2382-

436   2386.

437   Tamagnini F, Scullion S, Brown JT, Randall AD. 2014. Low Concentrations of the Solvent Dimethyl

438   Sulphoxide Alter Intrinsic Excitability Properties of Cortical and Hippocampal Pyramidal

439   Cells. PLoS One.

440   Thumm W, Freitag D, Kettrup A. 1991. Determination and quantification of dimethyl sulphoxide by

441   HPLC. Chromatographia 32(9):461-462.

442   Xu W, Chellam S. 2005. Initial Stages of Bacterial Fouling during Dead-End Microfiltration†.

443   Environmental Science & Technology 39(17):6470-6476.

444   Zhou X, Liu Z, Shu Z, Ding W, Du P, Chung J, Liu C, Heimfeld S, Gao D. 2011. A dilution-filtration

445   system for removing cryoprotective agents. J Biomech Eng 133(2):021007.

446

447

448   **Table Legends**

449   **Table 1** – Fixed inputs and parameters for the operation of the filtration device.

450

451   **Table 2** – Viable cell recovery, volume reduction and cell suspension viability after the filtration

452   operation, under 2mL/min bottom flow for 24 minutes, without lateral flow, for the injection molded

453   version of the filtration device.

454

455   **Table 3** – Viable cell recovery, volume reduction and cell suspension viability using the M3

456   geometry, under 2 mL/min bottom flow for 24 min, without lateral flow.

18

457   **Figure Legends**

458   **Figure 1** – Filtration device design and fluid flow. A)- CAD drawing of the filtration device housing,

459   divided in a top and bottom part (A, top); when the device is assembled (A, bottom) the filter is

460   located between the two parts and the cell suspension is introduced into the bottom, where it is

461   washed, concentrated and loaded into a syringe (B, Supplementary videos). Panel C) depicts the fluid

462   flow in the device: for visualization purposes, a red dyed PBS solution was used to wash 1 mL of a

463   (transparent) cell-free CryoStor5 solution (the full video is available in Supplementary Video S2A).

464   This frame corresponds to t=1s in the wash process.

465   **Figure 2** – DMSO removal is enhanced by backflush frequency. The filter device was operated for 10

466   min in the wash mode with a 2 mL/min bottom flow rate and a 5 mL/min cross flow rate; after this

467   wash step and before the concentration step a backflush was performed to dislodge cells from the

468   filter membrane (see methods). The concentration of DMSO in the collected filtrate fractions

469   increases after backflush (A). The backflush step was repeated 3 times throughout the wash period

470   (3xbackflush) and compared to a single backflush after the wash step (1xbackflush) (B) for the

471   amount of DMSO left in the cell suspension (lower chamber, which contains the retentate) (C) and the

472   pressure difference generated in the lower chamber (D). ***, $p < 0.001$.

473   **Figure 3** – Lateral flow wash alone shows a limited DMSO reduction. The filter device was operated

474   for 10 minutes in the wash mode with a 2 mL/min bottom flow rate without cross flow (20 mL, n=3),

475   with a 5 mL/min lateral flow rate without bottom flow (Lateral 5 mL/min, n=3) and with a 2 mL/min

476   bottom flow rate and a 5 mL/min cross flow rate (2/5 flow, n=6). ***, $p < 0.001$ (Tukey's

477   multicomparison test).

478   **Figure 4** – Synergistic effect of the lateral and bottom flows. The presence of lateral flow during cell

479   washing yields a DMSO reduction profile described by a single exponential function, as predicted by

480   equation 1 (A, closed squares, n≥3 for all data points), whereas in the absence of the lateral flow, the

481   bottom flow wash does not fit the equation 1 model (A, closed circles, n≥3 for all data points). The

482   typical pressure profiles for these 2 wash modes show that the presence of cross flow also leads to

483   pressure build-up in the lower chamber, unlike the bottom flow only operation mode (B). To mimic

                                                                                                    19

484   the final thermoplastic product the bottom flow chamber geometry was injection molded (C, purple)

485   to fit a PMMA housing (C, gray).

486   **Figure 5** – Redesigning the filtration device for improved DMSO removal. The original filtration

487   device was redesigned by changing the geometry of the bottom chamber which holds the cell

488   suspension, which led to changes in the distance between the bottom inlet and the filter membrane,

489   and filtration area (A). A CFD analysis on the M2 geometry revealed "dead zones" where the DMSO

490   was being removed with less efficiency (B). The 3 different geometries were evaluated for their

491   DMSO reduction capability (C, n≥3 for all data points), operated with (open symbols) and without

492   (closed symbols) lateral flow, except for M3, where lateral flow lead to clogging (data not shown); the

493   final pressure in the lower chamber, after 24 min, also revealed differences between geometries and

494   wash modes (D, n=3 for all data points). The sine of the angle α, formed between the horizontal plane

495   and the lower chamber slope that connects the bottom and lateral inlets (E), is different between

496   devices; when the number of diavolumes is multiplied by the $\sin(\alpha)$, specific for each device, the

497   curves that obey equation1 in C follow a single exponential decay empirical model, as described by

498   equation 2 (F). The M3 geometry was assessed for its ability to reduce albumin-FITC by washing a

499   cell suspension for 24 minutes at 2mL/min bottom flow (G); furthermore, the cellular proliferation

500   after filtration processing, using the M3 geometry (n=4), was compared with post-centrifugation

501   processing (n=5) and fresh cell culture processing (i.e. cell counts during passaging, n=5) by

502   calculating the specific growth rate μ (day^{-1}).

503   **Figure 6 –** hMSC post filtration recovery, proliferation and characterization. hMSCs were processed

504   using the M3 geometry filtration device. The post filtration characterization after 3 cell runs

505   (generated from 2 donors) was performed according to the ISCT criteria: cell surface markers (Figure

506   6 A, individual flow cytometry histograms, and B, aggregate results from the 3 cell runs), adherence

507   to plastic (Figure 6E, scale bar=400 mm) and the capability for chondrogenic, osteogenic and

508   adipogenic differentiation (Figure 6G, H, scale bar=100 mm, and I, scale bar=50 mm, respectively).

509   The viable cell recovery, DMSO removal and hMSC growth rates after filtration are displayed in

510   Figure 6 C, D and F, respectively).

511   **Supplementary Figure 1 –** <u>Isopycnic gradient centrifugation of MRC-5 cells in CryoStor 5.</u> A cell

512   suspension of 10^7 MRC-5 cells and a set of density marker beads (Cospherix, CA, USA) were

513   centrifuged in parallel in a 5-layer CS5/Percoll (GE Healthcare) gradient. This gradient was

514   established by overlaying CS5/Percoll solutions, in two 50 mL tubes, at a decreasing concentration of

515   Percoll (50, 40, 30, 20 and 10%); after overlaying the cell or marker bead CS5 suspension, the two

516   tubes were centrifuged at 4ºC for 30 min without acceleration or brake.

517   **Supplementary Figure 2 –** <u>Processor with the docked consumable (left) and the consumable only</u>

518   <u>(right) for the commercial version of the CPrep device.</u> The frozen cellular therapy is delivered from a

519   centralized manufacturing facility to the hospital. When a patient is ready the frozen vial is placed

520   into the CPREP consumable (yellow area), which is already docked to the processor. Here it is

521   thawed before being pumped into the novel filter device where the DMSO is washed out. After the

522   washing step the cells are drained into a syringe ready for administration. This entire fluidic circuit is

523   an integral part of the consumable.

524   **Supplementary Video S1A and S1B –** <u>Loading using the novel filtration device.</u> Video of the

525   loading process for CS5 with Alizarin Red (Supplementary Video 1A) and 10^7 MRC-5 cells

526   (Supplementary Video 1B).

527   **Supplementary Video S2A and S2B –** <u>Washing using the novel filtration device.</u> Video of the

528   washing process for PBS with Alizarin Red (Supplementary Video 2A, the dye has been dissolved in

529   PBS to visualize the jet flow from the bottom inlet to the membrane) and 10^7 MRC-5 cells

530   (Supplementary Video 2B).

531   **Supplementary Video S3A and S3B –** <u>Backflush using the novel filtration device.</u> Video of the

532   backflush process for CS5 with Alizarin Red (Supplementary Video 3A) and 10^7 MRC-5 cells

533   (Supplementary Video 3B).

534   **Supplementary Video S4 –** <u>Volume reduction using the novel filtration device.</u> Video of the volume

535   reduction process for CS5 containing 10^7 MRC-5 cells.

536

Table 1

Parameter/input	Value
Cell type	MRC-5 (lung fibroblast cell line)
Wash buffer	Phosphate buffered saline (PBS)
Cryopreservation solution	CryoStor-5 (5% DMSO)
Initial cell suspension volume	1 mL
Initial cell suspension concentration	10^7/mL
Cell chamber volume	1.5 mL
Total process time (w/o priming or manual steps)	$\leq$ 30min
Cell loading flow rate	2 mL/min
Lateral flow rate	5 mL/min
Backflush flow rate and time	5 mL/min for 10 sec (between wash and concentration)
Air flow rate (volume reduction)	1 mL/min

Fixed inputs and parameters for the operation of the filtration device.
254x190mm (96 x 96 DPI)

1
2
3
4
5
6
7
8
9
10
11
12
13
14
15
16
17
18
19
20
21
22
23
24
25
26
27
28
29
30
31
32
33
34
35
36
37
38
39
40
41
42
43
44
45
46
47
48
49
50
51
52
53
54
55
56
57
58
59
60

Table 2

| Run #	V_in (mL)	V_out (mL)	pre-process viable cell concentration (10^6/mL)	Input viability (%)	post-process viable cell concentration (10^6/mL)	Output viability (%)	Fold volume reduction	Total viable cell recovery (%)
1	1.086	0.393	15.5	89	36.1	92	2.8	84
2	0.821	0.408	12.1	88	20.1	91	2	83
3	1.052	0.334	10.8	91	28.8	94	3.1	85
4	0.952	0.322	10.9	88	27.5	92	3	85
Average	1.0	0.36	12	89	28	92	2.7	84
stdev	0.1	0.04	2	1	7	1	0.5	1
rel stdev (%)	10	11	17	1	25	1	19	1

Viable cell recovery, volume reduction and cell suspension viability after the filtration operation, under 2mL/min bottom flow for 24 minutes, without lateral flow, for the injection molded version of the filtration device.
254x190mm (96 x 96 DPI)

1
2
3
4
5
6
7
8
9
10
11
12
13
14
15
16
17
18
19
20
21
22
23
24
25
26
27
28
29
30
31
32
33
34
35
36
37
38
39
40
41
42
43
44
45
46
47
48
49
50
51
52
53
54
55
56
57
58
59
60

Table 3

M3 Run #	V_in (mL)	V_out (mL)	pre-process viable cell concentration (10^6/mL)	Input viability (%)	post-process viable cell concentration (10^6/mL)	Output viability (%)	Fold volume reduction	Total viable cell recovery (%)
1	1.03	0.68	9.7	70.2	13.6	89.1	1.52	92
2	1.00	0.66	10.2	86.6	14.1	89.1	1.52	91
3	0.96	0.65	10.2	89.0	15.7	89.0	1.49	103
4	1.04	0.62	9.3	83.4	14.1	85.9	1.69	89
5	0.92	0.61	8.8	89.5	12.4	87.8	1.51	93
Average	1.01	0.65	10	84	14	88	1.55	94
Std. dev.	0.04	0.03	1	8	1	1	0.08	5
C.V.(%)	4	5	10	10	7	1	5	5

Viable cell recovery, volume reduction and cell suspension viability using the M3 geometry, under 2 mL/min bottom flow for 24 min, without lateral flow.
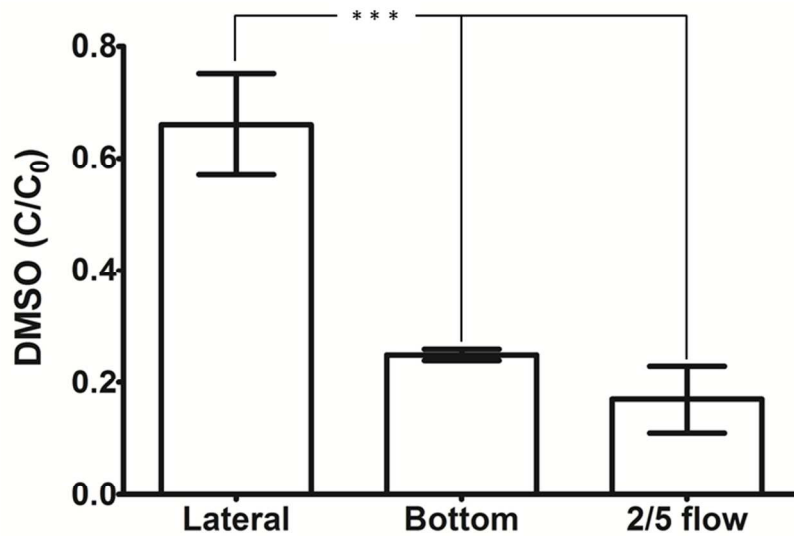254x190mm (96 x 96 DPI)
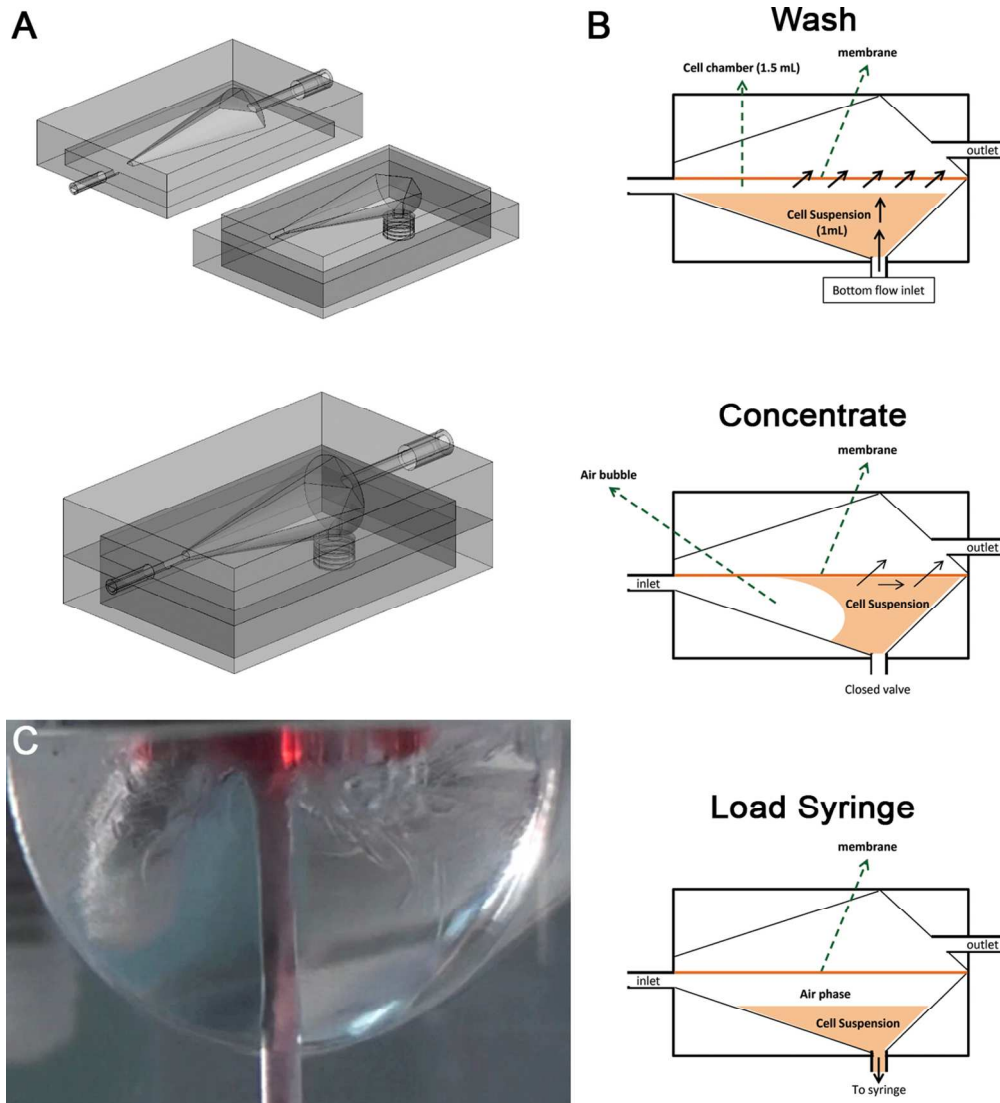
Filtration device design and fluid flow. A)- CAD drawing of the filtration device housing, divided in a top and bottom part (A, top); when the device is assembled (A, bottom) the filter is located between the two parts and the cell suspension is introduced into the bottom, where it is washed, concentrated and loaded into a syringe (B, Supplementary videos). Panel C) depicts the fluid flow in the device: for visualization purposes, a red dyed PBS solution was used to wash 1 mL of a (transparent) cell-free CryoStor5 solution (the full video is available in Supplementary Video S2A). This frame corresponds to t=1s in the wash process. 115x127mm (300 x 300 DPI)
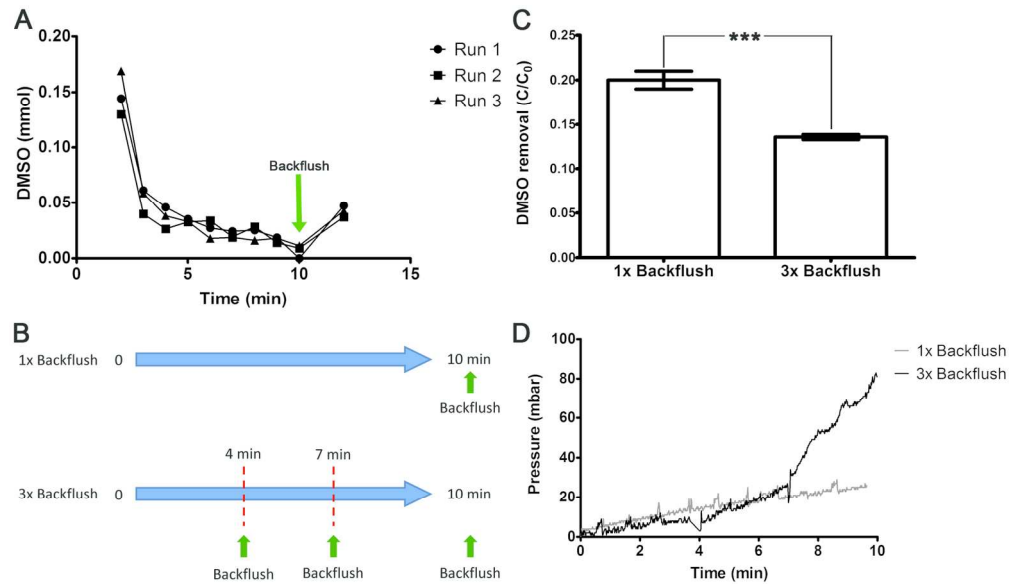
DMSO removal is enhanced by backflush frequency. The filter device was operated for 10 min in the wash mode with a 2 mL/min bottom flow rate and a 5 mL/min cross flow rate; after this wash step and before the concentration step a backflush was performed to dislodge cells from the filter membrane (see methods). The concentration of DMSO in the collected filtrate fractions increases after backflush (A). The backflush step was repeated 3 times throughout the wash period (3xbackflush) and compared to a single backflush after the wash step (1xbackflush) (B) for the amount of DMSO left in the cell suspension (lower chamber, which contains the retentate) (C) and the pressure difference generated in the lower chamber (D). ***, p<0.001. 160x94mm (300 x 300 DPI)

1
2
3
4
5
6
7
8
9
10
11
12
13
14
15
16
17
18
19
20
21
22
23
24
25
26
27
28
29
30
31
32
33
34
35
36
37
38
39
40
41
42
43
44
45
46
47
48
49
50
51
52
53
54
55
56
57
58
59
60

Lateral flow wash alone shows a limited DMSO reduction. The filter device was operated for 10 minutes in the wash mode with a 2 mL/min bottom flow rate without cross flow (20 mL, n=3), with a 5 mL/min lateral flow rate without bottom flow (Lateral 5 mL/min, n=3) and with a 2 mL/min bottom flow rate and a 5 mL/min cross flow rate (2/5 flow, n=6). ***, p<0.001 (Tukey's multicomparison test).
254x190mm (96 x 96 DPI)
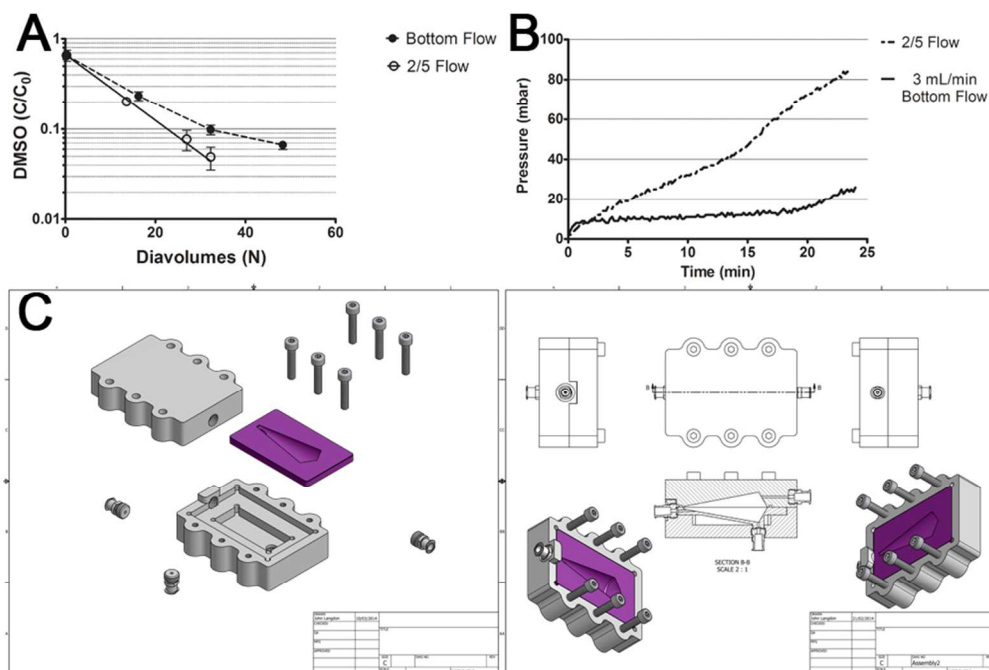
Synergistic effect of the lateral and bottom flows. The presence of lateral flow during cell washing yields a DMSO reduction profile described by a single exponential function, as predicted by equation 1 (A, closed squares, n≥3 for all data points), whereas in the absence of the lateral flow, the bottom flow wash does not fit the equation 1 model (A, closed circles, n≥3 for all data points). The typical pressure profiles for these 2 wash modes show that the presence of cross flow also leads to pressure build-up in the lower chamber, unlike the bottom flow only operation mode (B). To mimic the final thermoplastic product the bottom flow chamber geometry was injection molded (C, purple) to fit a PMMA housing (C, gray).
85x56mm (300 x 300 DPI)
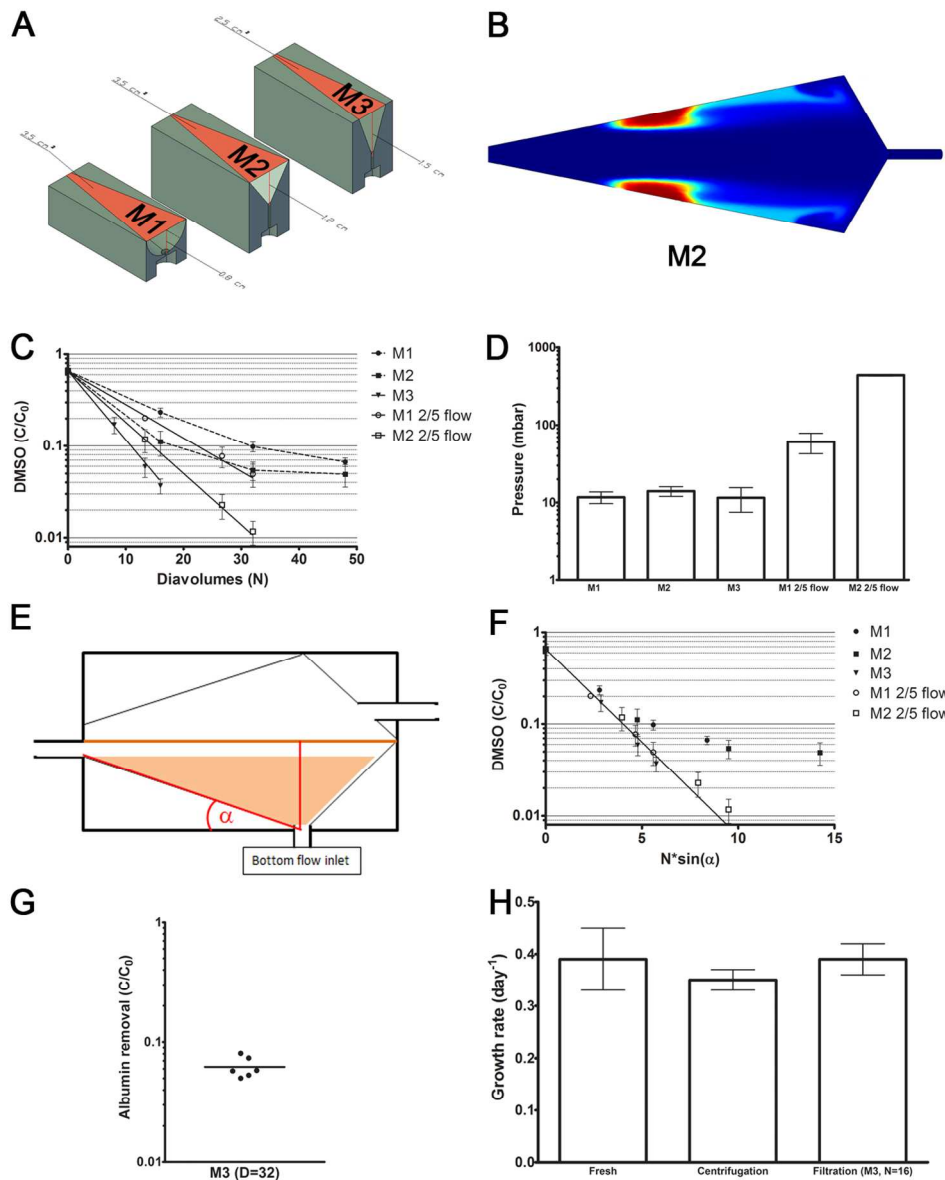
– Redesigning the filtration device for improved DMSO removal. The original filtration device was redesigned by changing the geometry of the bottom chamber which holds the cell suspension, which led to changes in the distance between the bottom inlet and the filter membrane, and filtration area (A). A CFD analysis on the M2 geometry revealed "dead zones" where the DMSO was being removed with less efficiency (B). The 3 different geometries were evaluated for their DMSO reduction capability (C, n≥3 for all data points), operated with (open symbols) and without (closed symbols) lateral flow, except for M3, where lateral flow lead to clogging (data not shown); the final pressure in the lower chamber, after 24 min, also revealed differences between geometries and wash modes (D, n=3 for all data points). The sine of the angle α, formed between the horizontal plane and the lower chamber slope that connects the bottom and lateral inlets (E), is different between devices; when the number of diavolumes is multiplied by the sin(α), specific for each device, the curves that obey equation1 in C follow a single exponential decay empirical model, as described by equation 2 (F). The M3 geometry was assessed for its ability to reduce albumin-FITC by washing a cell suspension for 24 minutes at 2mL/min bottom flow (G); furthermore, the cellular proliferation

after filtration processing, using the M3 geometry (n=4), was compared with post-centrifugation processing (n=5) and fresh cell culture processing (i.e. cell counts during passaging, n=5) by calculating the specific growth rate μ (day-1).
119x150mm (300 x 300 DPI)
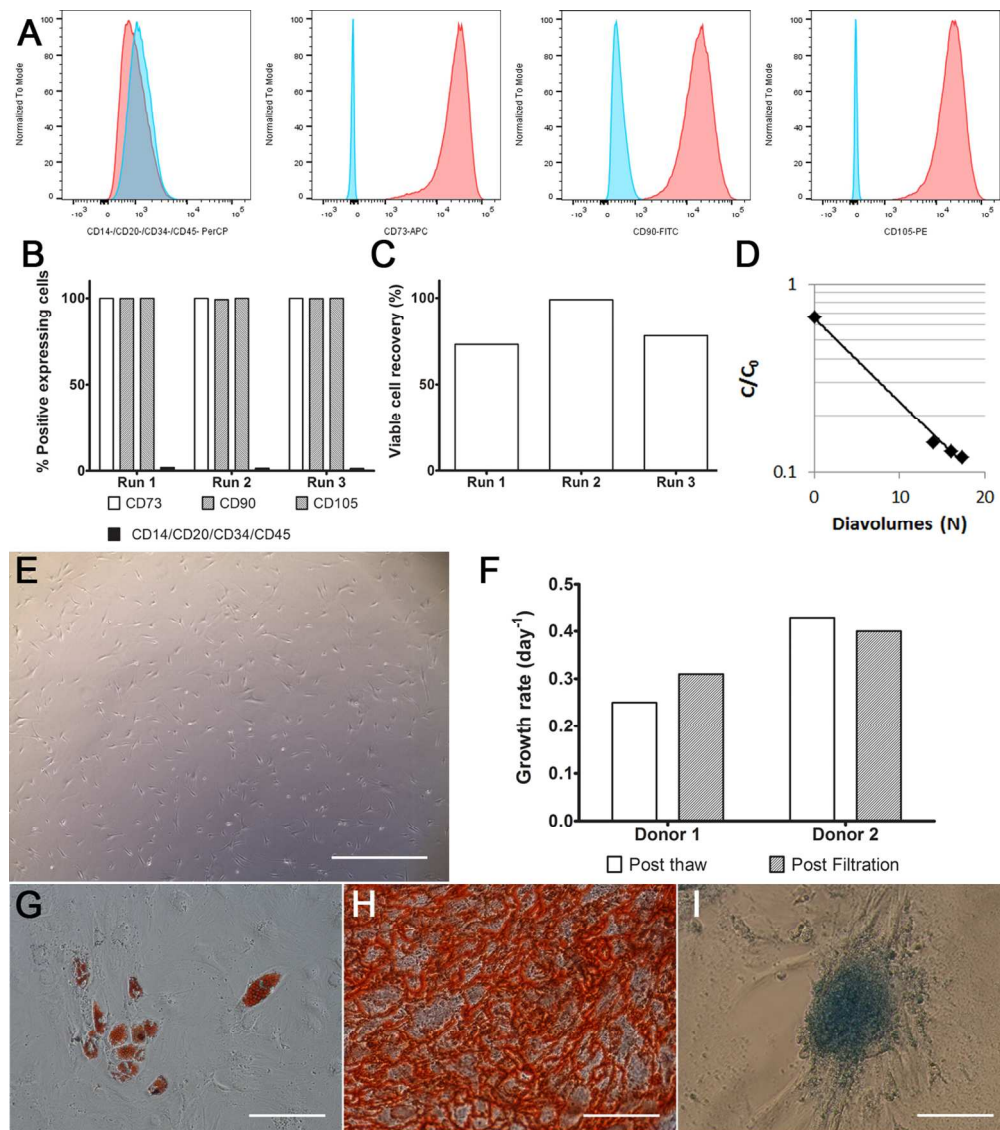
hMSC post filtration recovery, proliferation and characterization. hMSCs were processed using the M3 geometry filtration device. The post filtration characterization after 3 cell runs (generated from 2 donors) was performed according to the ISCT criteria: cell surface markers (Figure 6 A, individual flow cytometry histograms, and B, aggregate results from the 3 cell runs), adherence to plastic (Figure 6E, scale bar=400 µm) and the capability for chondrogenic, osteogenic and adipogenic differentiation (Figure 6G, H, scale bar=100 µm, and I, scale bar=50 µm, respectively). The viable cell recovery, DMSO removal and hMSC growth rates after filtration are displayed in Figure 6 C, D and F, respectively).
119x134mm (300 x 300 DPI)